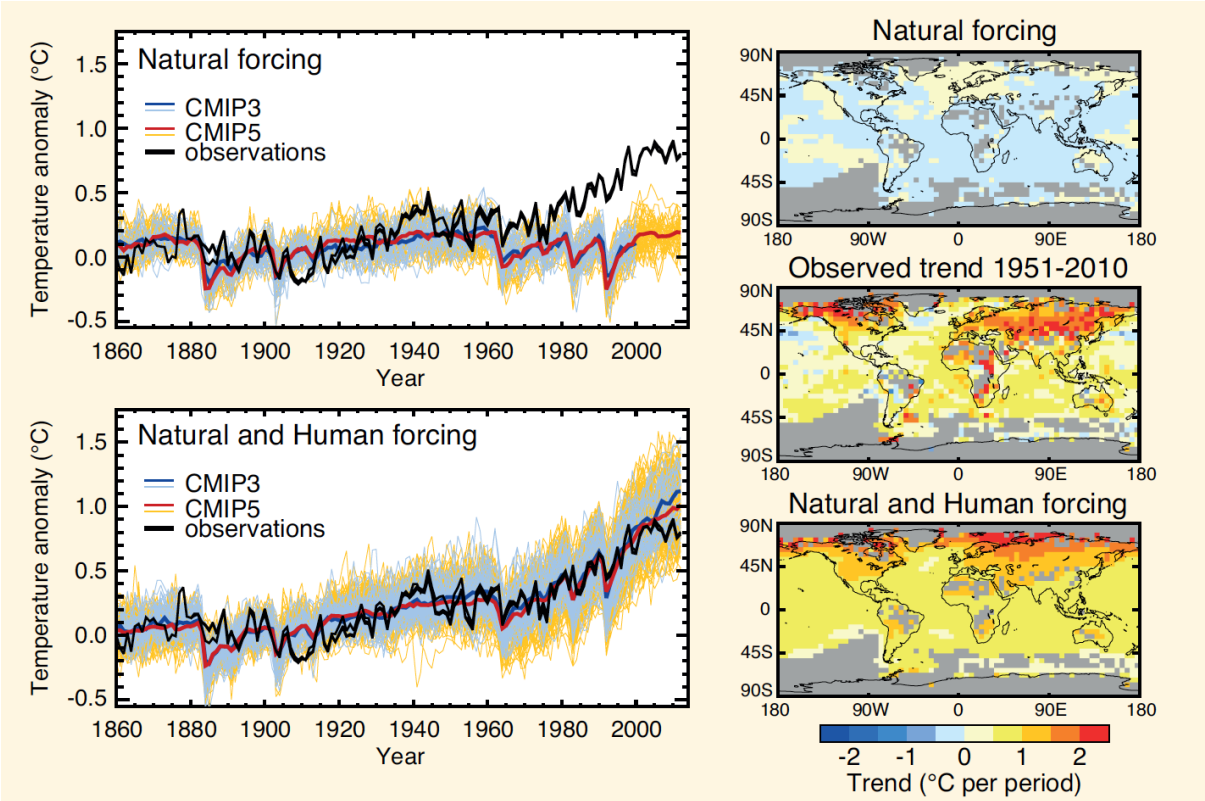

FAQ 10.1, Figure 1 | (Left) Time series of global and annual-averaged surface temperature change from 1860 to 2010. The top left panel shows results from two ensemble of climate models driven with just natural forcings, shown as thin blue and yellow lines; ensemble average temperature changes are thick blue and red lines. Three different observed estimates are shown as black lines. The lower left panel shows simulations by the same models, but driven with both natural forcing and human-induced changes in greenhouse gases and aerosols. (Right) Spatial patterns of local surface temperature trends from 1951 to 2010. The upper panel shows the pattern of trends from a large ensemble of Coupled Model Intercomparison Project Phase 5 (CMIP5) simulations driven with just natural forcings. The bottom panel shows trends from a corresponding ensemble of simulations driven with natural + human forcings. The middle panel shows the pattern of observed trends from the Hadley Centre/Climatic Research Unit gridded surface temperature data set 4 (HadCRUT4) during this period.

Figure S3.1: Attribution of global warming change (from IPCC AR5, Bindoff et al. 2013))

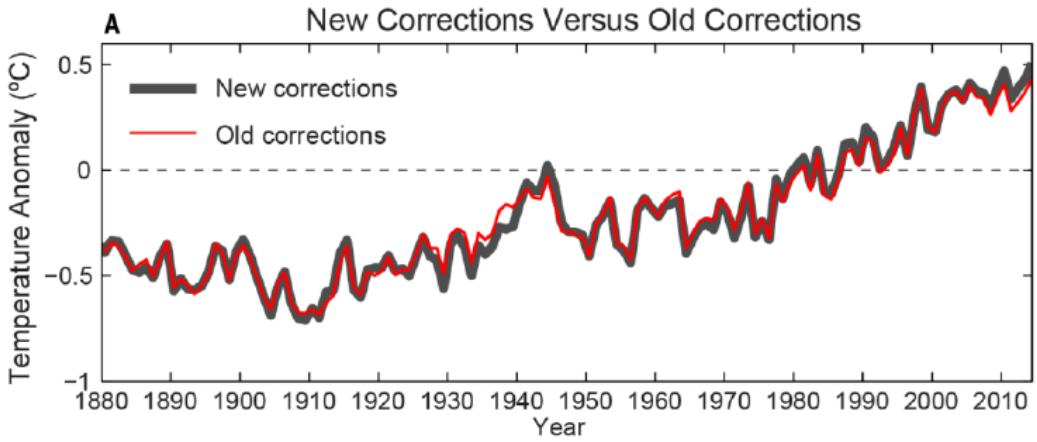

Figure S3.2 Global temperature warming using older and newer corrections (Karl et al. 2015)

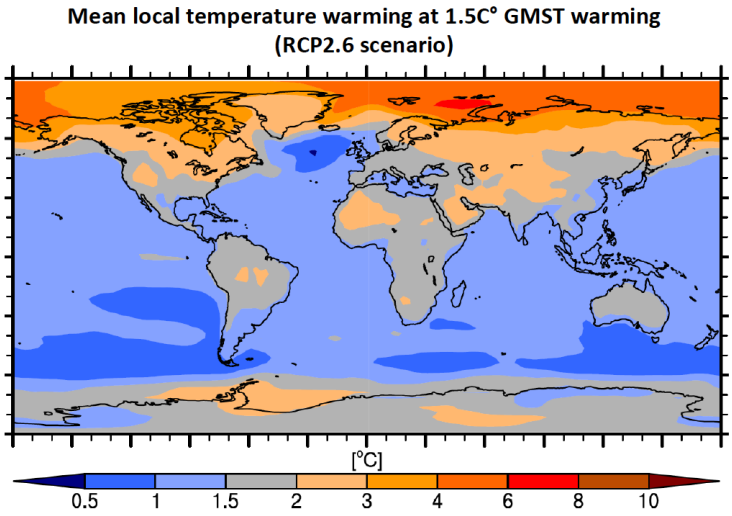

Figure S3.3 Same analysis as left-hand part of Fig. 3.4 but based on RCP2.6 scenario CMIP5 simulations.

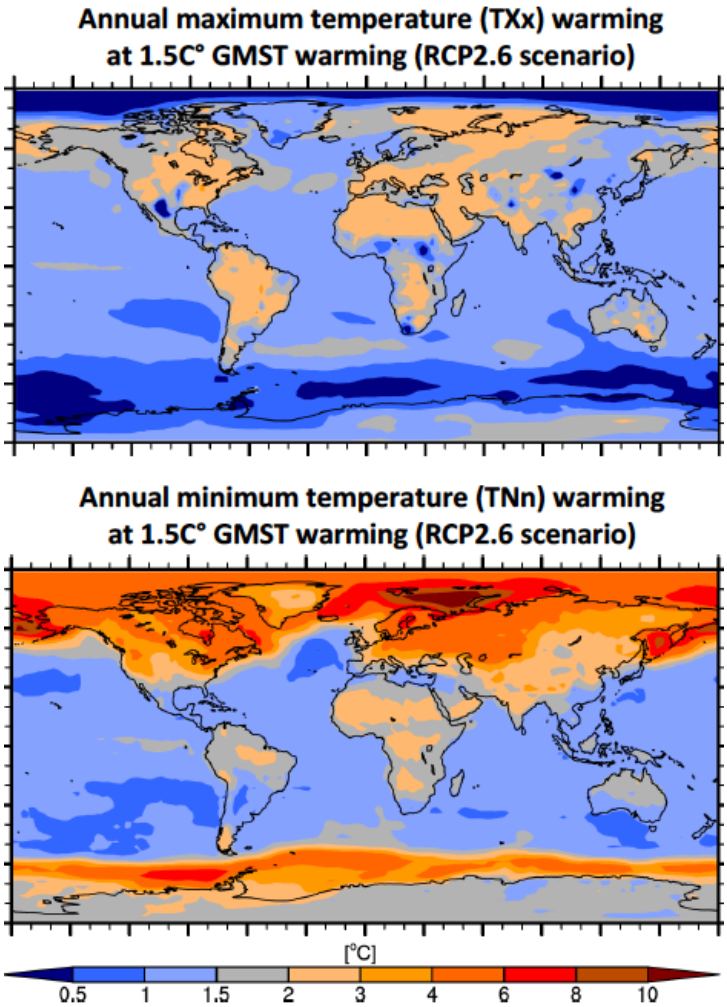

Figure S3.4 Same analysis as left-hand part of Fig. 3.5 but based on RCP2.6 scenario CMIP5 simulations

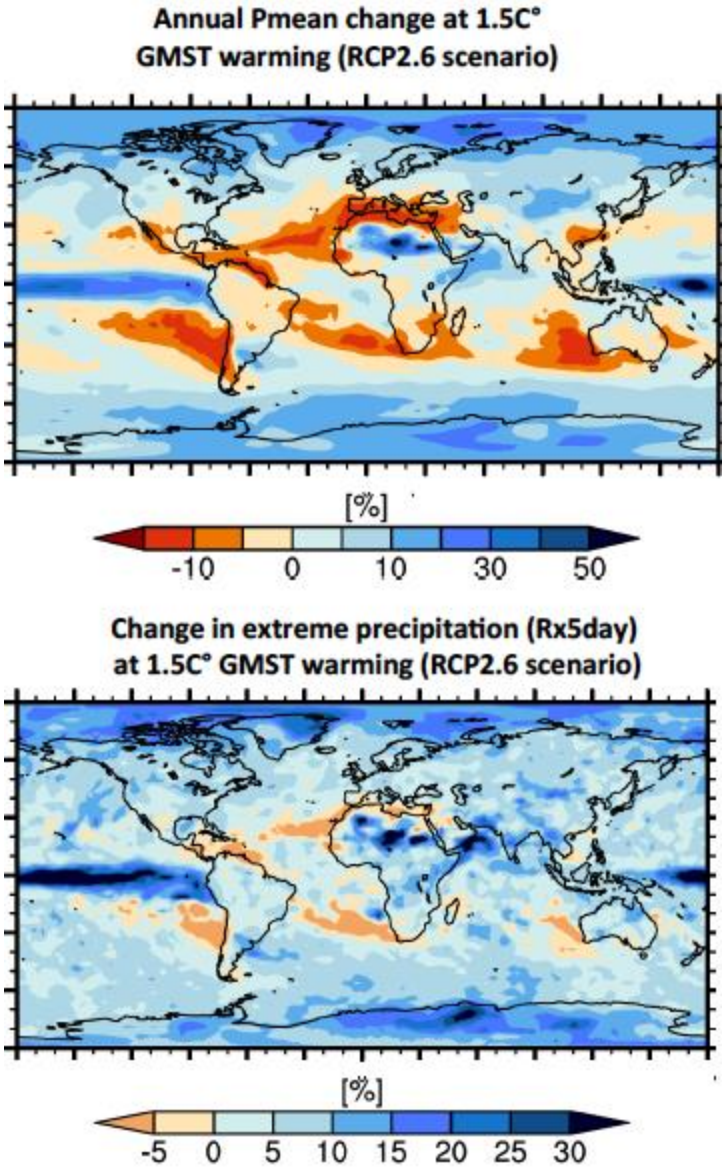

Figure S3.5 Same analysis as left-hand part of Fig. 3.6 but based on RCP2.6 scenario CMIP5 simulations

Table S3.1

See excel document: CH3_SM_TS3.1

Table S3.2

See excel document: CH3_SM_TS3.2

Table S3.3: Key economic sectors

Sector (sub sector)	*Region*	*Metric*	*Baselines*	*Climate model(s)*	*Scenario*	*Time periods of interest*	*Impacts at baseline*	*Projected impacts at 1.5℃*	*Projected impacts at 2℃*	*Other factors considered*	*Reference*
Energy (Electricity demand)	US	Electric sector models: GCAM-USA ReEDS IPM		MIT IGSM-CAM	REF CS3 REF CS6 POL4.5 CS3 POL3.7 CS3 TEMP 3.7 CS3	2015-2050			Increase in electricity demand by 1.6 to 6.5 % in 2050		McFarland et al. 2015
Energy (Hydropower)	US (Florida)	Conceptual rainfall-runoff (CRR) model: HYMOD MOPEX	1971-2000	CORDEX (6 RCMs) CMIP5, bias corrected	RCP4.5	2091-2100			Based on a min/max temp. increase of 1.35°-2°C, overall stream flow to increase by an average of 21% with pronounced seasonal variations, resulting in increases in power generation (72%		Chilkoti et al. 2017

Sector (sub sector)	*Region*	*Metric*	*Baselines*	*Climate model(s)*	*Scenario*	*Time periods of interest*	*Impacts at baseline*	*Projected impacts at 1.5℃*	*Projected impacts at 2℃*	*Other factors considered*	*Reference*
									winter, 15% autumn) and decreasing (-14%) in summer		
Energy (Hydropower)	Global	Gross hydropower potential; global mean cooling water discharge	1971-2000	5 bias-corrected GCMs	RCP2.6 RCP8.5	2080			Global gross hydropower potential expected to increase (+2.4% RCP2.6; +6.3% RCP8.5) Strongest increases in central Africa, Asia, India, and northern high latitudes. 4.5-15% decrease in global mean	Socio-economic pathways	van Vliet et al. 2016

Sector (sub sector)	*Region*	*Metric*	*Baselines*	*Climate model(s)*	*Scenario*	*Time periods of interest*	*Impacts at baseline*	*Projected impacts at 1.5℃*	*Projected impacts at 2℃*	*Other factors considered*	*Reference*
									cooling water discharge with largest reductions in US and Europe		
Energy (Hydropower)	Brazil	Hydrological Model for natural water inflows (MGB)	1960-1990	HadCM3 Eta-CPTEC-40		2011-2100		A decrease in electricity generation of about 15% and 28% for existing and future generation systems starting in 2040		Other water use and economic development scenarios	de Queiroz et al. 2016
Energy (Wind)	Europe	Near surface wind data: Wind energy density means; Intra and inter annual variability	1986-2005	21 CMIP5 Euro-CORDEX	RCP8.5 RCP4.5	2016-2035 2046-2065 2081-2100		No major differences in large scale wind energetic resources, inter-annual or intra-annual variability in near term future (2016-2035)	Decreases in wind energy density in eastern Europe, Increases in Baltic regions (-30% vs. +30%). Increase of intra-	Changes in wind turbine technology	Carvalho et al. 2017

Sector (sub sector)	*Region*	*Metric*	*Baselines*	*Climate model(s)*	*Scenario*	*Time periods of interest*	*Impacts at baseline*	*Projected impacts at 1.5℃*	*Projected impacts at 2℃*	*Other factors considered*	*Reference*
									annual variability in Northern Europe, decrease in Southern. Inter-annual variability not expected to change		
Tourism	Europe	Climate Index for Tourism; Tourism Climatic Index (3 variants)		Euro-CORDEX	RCP4.5 RCP8.5	+2° C			Varying magnitude of change across different indices; Improved climate comfort for majority of areas for May to October period; June to August period climate		Grillakis et al. 2016

Sector (sub sector)	*Region*	*Metric*	*Baselines*	*Climate model(s)*	*Scenario*	*Time periods of interest*	*Impacts at baseline*	*Projected impacts at 1.5℃*	*Projected impacts at 2℃*	*Other factors considered*	*Reference*
									favorability projected to reduce in Iberian peninsula due to high temperatures		
Tourism	Southern Ontario (Canada)	Weather-visitation models (peak, shoulder, off-season)				1° to 5° C warming		Each additional degree of warming experienced annual park visitation could increase by 3.1%, annually.		Social variables e.g. weekends or holidays	Hewer et al. 2016
Tourism	Europe	Natural snow conditions (VIC); Monthly overnight stay; Weather Value at Risk	1971-2000	Euro-CORDEX	RCP2.6 RCP4.5 RCP8.5	+2°C periods: 2071-2100 2036-2065 2026-2055			Under a +2°C global warming up to 10 million overnight stays are at risk (+7.3 million nights) Austria and Italy are	Tourism trends based on economic conditions	Damm et al. 2016

Sector (sub sector)	*Region*	*Metric*	*Baselines*	*Climate model(s)*	*Scenario*	*Time periods of interest*	*Impacts at baseline*	*Projected impacts at 1.5℃*	*Projected impacts at 2℃*	*Other factors considered*	*Reference*
									most affected.		
Tourism	Sardinia (Italy) and the Cap Bon peninsula (Tunisia)	Overnight stays; weather/climate data (E-OBS)	1971-2000	EU-FP6 ENSEMBLES (ECH-REM, ECH-RMO, HCH-RCA and ECH-RCA)		2041-2070			Climate-induced tourism revenue gains especially in the shoulder seasons during spring and autumn; threat of climate-induced revenue losses in the summer months due to increased heat stress.	GDP; Prices, Holidays; Events	Köberl et al. 2016
Tourism	Iran (Zayandehroud River route)	Physiologically equivalent temperature (PET)	1983-2013	HADCM3	B1 A1B	2014-2039		The PET index shows a positive trend with a reduction in number of			Yazdanpanah et al. 2016

Sector (sub sector)	*Region*	*Metric*	*Baselines*	*Climate model(s)*	*Scenario*	*Time periods of interest*	*Impacts at baseline*	*Projected impacts at 1.5℃*	*Projected impacts at 2℃*	*Other factors considered*	*Reference*
								climate comfort days (18 < PET < 29), particularly in the western area			
Tourism	Portugal	Arrivals of inbound tourists; GDP						Increasing temperatures are projected to lead to a decrease of inbound tourism arrivals between 2.5% and 5.2%, which is expected to reduce Portuguese GDP between 0.19% and 0.40%.			Pintassilgo et al. 2016
Transportation (shipping)	Arctic Sea (north sea route)	Climatic loses; Gross gains; Net gains		PAGE-ICE	RCP4.5 RCP8.5 SSP2	2013-2200		Large-scale commercial shipping is unlikely possible until 2030 (bulk) and 2050 (container) under RCP8.5.	The total climate feedback of NSR could contribute 0.05% to global mean temperatur	Business restrictions	Yumashev et al. 2017

Sector (sub sector)	*Region*	*Metric*	*Baselines*	*Climate model(s)*	*Scenario*	*Time periods of interest*	*Impacts at baseline*	*Projected impacts at 1.5℃*	*Projected impacts at 2℃*	*Other factors considered*	*Reference*
									e rise by 2100 under RCP8.5 adding $2.15 Trillion to the Net Present Value of total impacts of climate change over the period until 2200. The climatic losses offset 33% of the total economic gains from NSR under RCP8.5 with the biggest losses set to occur in Africa and India.		

Sector (sub sector)	*Region*	*Metric*	*Baselines*	*Climate model(s)*	*Scenario*	*Time periods of interest*	*Impacts at baseline*	*Projected impacts at 1.5℃*	*Projected impacts at 2℃*	*Other factors considered*	*Reference*
Transportation (air)	Global (19 major airports)	Takeoff weight (TOW) restrictions	1985-2005	CMIP5	RCP4.5 RCP8.5	2060-2080			On average, 10–30% of annual flights departing at the time of daily maximum temperature may require some weight restriction below their maximum takeoff weights which may impose increased cost on airlines	Improved aircraft or airport design	Coffel et al. 2017
Water	Europe	Runoff Discharge Snowpack based on hydrological models:		CMIP5 CORDEX (11) Bias corrected to E-OBS	RCP2.6 RCP4.5 RCP8.5	1.5° C 2° C 3° C		Increases in runoff affect the Scandinavian mountains; Decreases in	Increases in runoff in Norway, Sweden, & N. Poland; Decreases		Donnelly et al. 2017

Sector (sub sector)	*Region*	*Metric*	*Baselines*	*Climate model(s)*	*Scenario*	*Time periods of interest*	*Impacts at baseline*	*Projected impacts at 1.5℃*	*Projected impacts at 2℃*	*Other factors considered*	*Reference*
		E-HYPE Lisflood WBM LPJmL						runoff in Portugal	in runoff around Iberian, Balkan, and parts of French coasts.		
Water	Global (8 river regions)	River runoff Glob-HM Cat-HM		HadGEM2-ES IPSL-CM5A-LR; MIROCESM-CHEM; GFDL-ESM2; NorESM1-M;	RCP8.5	1° C 2° C 3° C 1971-2099		Projected runoff changes for the Rhine (decrease), Tagus (decrease) and Lena (increase) with global warming	Increased risk of decreases in low flows (Rhine) (−11% at 2 °C to −23% at 3 °C) Risk of increases in high flows increases for Lena +17% (2 °C) to +26% (3 °C)		Gosling et al. 2017

Table S3.4: Projected temperature-related risks to human health

Region	*Health outcome metric*	*Baselines*	*Climate model(s)*	*Scenario*	*Time periods of interest*	*Impacts at baseline*	*Projected impacts at 1.5°C*	*Projected impacts at 2°C*	*Other factors considered*	*Reference*
Global and 21 regions	Heat-related mortality in adults over 65 years of age	1961-1990	BCM2.0; EGMAM1; EGMAM2; EGMAM3; CM4vl	A1B	2030; 2050		In 2030, 92,207 additional heat-related deaths without adaptation and (ensemble mean) and 37,588 with adaptation under BCM2 scenario; the Asia Pacific, Asia, North Africa / Middle East, Sub-Saharan Africa, Europe, and north America at higher risk.	In 2050, 255,486 additional heat-related deaths without adaptation and 73,936 with adaptation under BCM2 scenario; the same regions are at higher risk.	Population growth and aging; improved health in elderly due to economic development; three levels of adaptation (none, partial, and full)	Hales et al. 2014
Global	Heatwave area calculated as the area with heatwaves divided by the total land area; number of heatwave days	1971-2000	HadGEM2-ES, bias corrected, from ISIMIP	RCP2.6 with SSP1; RCP6.0 with SSP2; RCP8.5 with SSP3	2030-2050; 2080-2100		Number of heatwave days approximately doubles by 2030-2040, with higher risk under RCP8.5-SSP3. Under	Number of heatwave days increases rapidly by 2080-2100, with the magnitude of increase varying across	Population density, % of population over 65 years of age; per capita GDP; education levels	Dong et al. 2015

Region	*Health outcome metric*	*Baselines*	*Climate model(s)*	*Scenario*	*Time periods of interest*	*Impacts at baseline*	*Projected impacts at 1.5°C*	*Projected impacts at 2°C*	*Other factors considered*	*Reference*
							RCP6.0-SSP2, the general spatial risk distribution is similar to RCP8.5-SSP3, but the average risk is lower. Very high-risk areas are in Africa and Asia.	regions, with higher risk under RCP8.5-SSP3. Very high-risk areas are in Europe, West Asia, East Asia, and North America. Under RCP6.0-SSP2, the general spatial risk distribution is similar, but the average risk is lower.		
Global	Extremely hot summers over land areas (>3 SD anomalies)	1861-1880	26 models from CMIP5	RCP2.6; RCP4.5; RCP8.5	to 2100s	Probability of an extremely hot summer (>3 sigma) in 1996-2005 (compared with 1951-1980) is 4.3%	Probability of an extremely hot summer is approximately 25.5% and probability of an exceedingly hot summer (>5 sigma) is approximately	Extremely hot summers are projected to occur over nearly 40% of the land area		Wang et al. 2015

Region	*Health outcome metric*	*Baselines*	*Climate model(s)*	*Scenario*	*Time periods of interest*	*Impacts at baseline*	*Projected impacts at 1.5°C*	*Projected impacts at 2°C*	*Other factors considered*	*Reference*
							7.1% above pre-industrial			
Australia (five largest cities) and UK	Temperature-related mortality	1993-2006	UKCP09 from HadCM3; OzClim 2011	A1B, B1, A1FI	2020s; 2050s; 2080s	For England and Wales, the estimated % change in mortality associated with heat exposure is 2.5% (95% CI: 1.9 - 3.1) per 1°C rise in temperature above the heat threshold (93rd %ile of daily mean temperature). In Australian cities, the estimated overall % change in mortality is 2.1% (95% CI: 1.3, 2.9).	In the 2020s, heat-related deaths increase from 1,503 at baseline to 1,511 with a constant population and 1,785 with the projected population. In Australia, the numbers of projected deaths are 362 and 475, respectively, with a baseline of 214 death.	In the 2050s, heat-related deaths further increase to 2,866 with a constant population and to 4.012 with the projected population. In Australia, the numbers of projected deaths are 615 and 970, respectively.	Projected population change	Vardoulakis et al. 2014
Australia	Temperature-related morbidity and	1971-2000	CSIRO	2030 A1B low and high; 2070	2030; 2070	4-6 dangerously hot days per	Sydney - from 3.5 days at baseline to	Sydney – 6-12 days and		Hanna et al. 2011

Region	*Health outcome metric*	*Baselines*	*Climate model(s)*	*Scenario*	*Time periods of interest*	*Impacts at baseline*	*Projected impacts at 1.5°C*	*Projected impacts at 2°C*	*Other factors considered*	*Reference*
	mortality; days per year above 35°C			A1FI low and high		year for un-acclimatized individuals	4.1-5.1 days in 2030; Melbourne - from 9 days at baseline to 11-13 days in 2030	Melbourne – 15-26 in 2070		
Brisbane, Sydney, and Melbourne Australia	Temperature-related mortality	1988-2009	62 GCMs, with spatial downscaling and bias correction	A2, A1B, B1	2050s; 2090s		In 2030, net temperature-related mortality (heat – cold) increases in Brisbane under all scenarios, increases in Sydney under A2, and declines in Melbourne under all scenarios	In 2090, there are further net temperature-related mortality (heat – cold) increases in Brisbane under all scenarios, increases in Sydney under A2 and A1B, and further declines in Melbourne under all scenarios		Guo et al. 2016
Brisbane Australia	Years of life lost due to temperature extremes (hot and cold)	1996-2003		Added 1 to 4C to observed daily temperatur	2000; 2050	In 2000, 3,077 temperature-related years of life lost for men, with 616 years of life		For 1C above baseline, years of life lost increase by 1,014 (840-1,178) for hot		Huang et al. 2012

Region	*Health outcome metric*	*Baselines*	*Climate model(s)*	*Scenario*	*Time periods of interest*	*Impacts at baseline*	*Projected impacts at 1.5°C*	*Projected impacts at 2°C*	*Other factors considered*	*Reference*
				e to project for 2050		lost due to hot temperatures and 2,461 years of life lost due to cold. The numbers for women are 3,495 (total), 903 (hot), and 2,592 (cold).		temperatures and decrease by 1,112 (-1,337 to -871) for cold temperatures		
Quebec, Canada	Heat-related mortality	1981-1999	Ouranos Consortium ; SDSM downscaled HADCM3	A2 and B2 (projected impacts the same)	2020 (2010 – 2039); 2050 (2040 – 2069); 2080 (2070 – 2099)		2% increase in summer mortality in 2020	4-6% increase in summer mortality in 2050		Doyon et al. 2008
Montreal, Canada	Heat-related mortality	June – August 1990 - 2007	Canadian Global Circulation Model, 3.1; CSIRO Mark 3.5; ECHAM5; MRRC (Canadian regional	B1, A1B, A2	June-August 2020-2037	55 (95% CI = 32-79) attributed deaths during June-August	Temperature-related mortality during June-August more than doubled for Tmax (78-161 deaths)		Assumed no change in mean daily death count; no demographic change; no change in ozone levels; no adaptation	Benmarhnia et al. 2014

Region	*Health outcome metric*	*Baselines*	*Climate model(s)*	*Scenario*	*Time periods of interest*	*Impacts at baseline*	*Projected impacts at 1.5°C*	*Projected impacts at 2°C*	*Other factors considered*	*Reference*
			climate model)							
USA	Heat-related mortality	1999-2003	GISS-II downscaled using MM5	A1B	2048-2052			For 2048-2052, May-September excess heat-related mortality projected to be 3700-3800 from all causes and 21,000 – 27,000 from non-accidental deaths	Projected population change	Voorhees et al. 2011
USA	Avoided climate impacts of heatwaves and cold spells	1981-2005	CESM-LE with RCP8.5; CEMS-ME with RCP4.5. Includes urban heat island effect	RCP4.5; RCP8.5	2061-2080	Mean annual total heatwave days range from 4.4-6.3; similar range for cold spells		In 2061-2080, urban annual heatwave days increase up to 92 (southeast) in RCP8.5. Following RCP4.5 reduces heat wave days by about 50 %. Large avoided impacts are		Oleson et al. 2015

Region	*Health outcome metric*	*Baselines*	*Climate model(s)*	*Scenario*	*Time periods of interest*	*Impacts at baseline*	*Projected impacts at 1.5°C*	*Projected impacts at 2°C*	*Other factors considered*	*Reference*
								demonstrated for individual communities. Heatwaves also start later in the season under RCP4.5.		
USA, 209 cities	Heat- and cold-related mortality	1990 (1976-2005)	Bias corrected (BCCA) GFDL-CM3; MIROC5	RCP6.0	2030 (2016-2045); 2050 (2036-2065); 2100 (2086-2100)		In 2030, a net increase in premature deaths, with decreases in temperature-related winter mortality and increases in summer mortality; the magnitude varied by region and city with an overall increase of 11,646 heat-related deaths.	In 2050, a further increase in premature deaths, with decreases in temperature-related winter mortality and increases in summer mortality; the magnitude varied by region and city with an overall increase of 15,229 heat-related deaths. In 2100, 27,312 heat-	Held population constant at 2010 levels; mortality associated with high temperatures decreased between 1973-1977 and 2003-2006	Schwartz et al. 2015

Region	*Health outcome metric*	*Baselines*	*Climate model(s)*	*Scenario*	*Time periods of interest*	*Impacts at baseline*	*Projected impacts at 1.5°C*	*Projected impacts at 2°C*	*Other factors considered*	*Reference*
								related deaths are projected.		
USA, 209 cities	Mortality associated with cold spells	1960-2050	CMIP5; 20 biased corrected (BCCAv2) multi-model dataset	RCP2.6; RCP4.5; RCP6.0; RCP8.5	1960-2050			Small decrease in projected mortality risk from 1960 to 2050, with significant variation across regions	Assumed no change in demography or baseline mortality rate	Wang et al. 2016
USA, 82 communities	High-mortality heatwaves that increase mortality by 20%	1981-2005	CESM-LE with RCP85; CESM-ME with RCP4.5	RCP4.5; RCP8.5	2061-2080	Depending on modeling approach, 5-6 high mortality heatwaves annually, with approximately 2 million person-days of exposure per year		At least seven more high-mortality heatwaves expected in a twenty-year period in the study communities under RCP8.5 than RCP4.5 when assuming no adaptation. Projections are most strongly influenced by the adaptation scenario.	Projected population change (SSP3, SSP5) and three scenarios of adaptation (no, lagged, on pace)	Anderson et al. 2016

Region	*Health outcome metric*	*Baselines*	*Climate model(s)*	*Scenario*	*Time periods of interest*	*Impacts at baseline*	*Projected impacts at 1.5°C*	*Projected impacts at 2°C*	*Other factors considered*	*Reference*
Washington State, USA	Heat-related mortality	1970-1999	PCM1; HadCM	Average of PCM1-B1 and HadCM-A1B; humidex baseline; number & duration of heatwaves calculated	2025; 2045; 2085		Under moderate warming in 2025, 96 excess deaths in Seattle area	Under moderate warming in 2045, 156 excess deaths in Seattle area; in 2085, 280 excess deaths	Holding population constant at 2025 projections	Jackson et al. 2010
Eastern USA	Heat-related mortality	2002-2004	CESM1.0 downscaled using WRF	RCP 4.5; RCP 8.5	2057-2059	187 $\pm$ 173 (2, 614) annual deaths in 2002-2004		Excess mortality attributable to heatwaves could result in 200-7,807 deaths / year under RCP8.5; average excess mortality is 1,403 deaths/year under RCP4.5 and 3,556 under RCP8.5	Projected population change in 2050	Wu et al. 2014
Rhode Island, USA	Heat-related emergency department admissions	2005-2012	CMIP5 multi-model ensemble bias	RCP 4.5; RCP 8.5	2046-2053; 2092-2099;	Between 2005 and 2012, an increase in maximum	Under RCP8.5, in 2046-2053, there would be	Under RCP8.5, in 2092–2099, there would be	Population and other	Kingsley et al. 2016

Region	*Health outcome metric*	*Baselines*	*Climate model(s)*	*Scenario*	*Time periods of interest*	*Impacts at baseline*	*Projected impacts at 1.5°C*	*Projected impacts at 2°C*	*Other factors considered*	*Reference*
	and heat-related morality		corrected (BCCA)		projections for April - October	daily temperature from 75 to 85F is associated with 1.3% and 23.9% higher rates of all cause and heat-related emergency department visits. Between 1999-2011, there is a 4.0% increase in heat-related mortality.	about 0.5% and 6.8% more all-cause and heat-related ED admissions, respectively, and 0.7% more deaths annually. Risks are lower under RCP4.5.	1.2% and 24.4% more all-cause and heat-related ED admissions, respectively, and 1.6% more deaths annually. Risks are lower under RCP4.5.	factors held constant	
Boston, New York, Philadelphia, USA	Heat-related mortality	1971-2000	CMIP5 bias corrected (BCSD)	RCP 4.5; RCP 8.5	2010 – 2039; 2040 – 2069; 2070 - 2099	Baseline heat-related mortality is 2.9 – 4.5 / 100,000 across the three cities	In the 2020s under both RCPs, heat-related mortality increased to 5.9 – 10 / 100,000	In the 2050s, heat-related mortality increased to 8.8 – 14.3 / 100,000 under RCP4.5 and to 11.7 to 18.9 / 100,000 under RCP8.5	Population constant at 2000	Petkova et al. 2013
New York City, NY	Heat-related mortality	Each model's	Downscaled and bias	RCP 4.5; RCP 8.5	2020s (2010-	638 heat-related deaths		Median projected	Five scenarios of	Petkova et al. 2017

Region	*Health outcome metric*	*Baselines*	*Climate model(s)*	*Scenario*	*Time periods of interest*	*Impacts at baseline*	*Projected impacts at 1.5°C*	*Projected impacts at 2°C*	*Other factors considered*	*Reference*
		30-year baseline average	corrected (BCSD) WCRP CMIP5, including 33 GCMs		2039); 2050s (2040-2069); 2080s (2070-2099)	annually between 2000 and 2006. Heat-related mortality relatively constant during the first part of the 20th century, then decreased from the 1970s to 2000s.		annual heat-related deaths varied greatly by RCP, adaptation, and population change scenario, ranging from 167 to 3,331 in the 2080s	population projections by gender; two adaptation scenarios plus no adaptation scenario	
Houston, Texas	Heat-related non-accidental mortality	1991-2010	CESM simulations for RCP8.5 and for RCP4.5; used HRLDAS for downscaling	RCP45; RCP8.5	2061-2080			Median annual non-accidental mortality under RCP4.5 about 50% less than under RCP8.5. For RCP4.5, 5,032 deaths under SSP3 and 7,935 deaths under SSP5. For RCP8.5, 5,130 deaths under SSP3 and	Demographics and income in SSP3 and SSP5; urban heat island	Marsha et al. 2016

Region	*Health outcome metric*	*Baselines*	*Climate model(s)*	*Scenario*	*Time periods of interest*	*Impacts at baseline*	*Projected impacts at 1.5°C*	*Projected impacts at 2°C*	*Other factors considered*	*Reference*
								8,079 deaths under SSP5.		
Europe	Heat-related respiratory hospital admissions	1981-2000	RCA3 dynamically downscaled results from CCCSM3, ECHAM5, HadCM3, ECHAM4	A1B; A2	2021-2050	The estimated proportion of respiratory hospital admissions due to heat is 0.18% at baseline in the EU27; the rate is higher for Southern Europe (0.23%). 11,000 respiratory hospital admissions across Europe in reference period		For all of Europe, 26,000 heat-related respiratory hospital admissions annually in 2021-2015. Southern Europe projected to have 3-times more heat attributed respiratory admissions.	Population projections	Astrom et al. 2013
UK	Temperature-related mortality	1993-2006	9 regional model variants of HadRm3-PPE-UK, dynamically downscaled	A1B	2000-2009; 2020-2029; 2050-2059; 2080-2089	At baseline, 1,974 annual heat-related and 41,408 cold-related deaths	In the 2020s, in the absence of adaptation, heat-related deaths would increase to 3,281 and cold-related deaths to	In the 2050s, the absence of adaptation, heat-related deaths projected to increase 257% by the 2050s to 7,040 and	Population projections to 2081	Hajat et al. 2014

Region	*Health outcome metric*	*Baselines*	*Climate model(s)*	*Scenario*	*Time periods of interest*	*Impacts at baseline*	*Projected impacts at 1.5°C*	*Projected impacts at 2°C*	*Other factors considered*	*Reference*
							increase to 42,842	cold-related mortality to decline about 2%		
Netherlands	Temperature-related mortality	1981-2010	KNMI' 14; G-scenario is a global temperature increase of 1°C and W-scenario an increase of 2°C		2050 (2035-2065)	At baseline, the attributable fraction for heat is 1.15% and for cold is 8.9%; or 1511 deaths from heat and 11,727 deaths from cold	Without adaptation, under the G scenario, the attributable fraction for heat is 1.7-1.9% (3329-3752 deaths) and for cold is 7.5-7.9% (15,020-15,733 deaths). Adaptation decreases the numbers of deaths, depending on the scenario.	Without adaptation, under the W scenario, the attributable fraction for heat is 2.2-2.5% (4380-5061 deaths) and for cold is 6.6-6.8% (13,149-13699 deaths). Adaptation decreases the numbers of deaths, depending on the scenario.	Three adaptation scenarios, assuming a shift in the optimum temperature, changes in temperature sensitivity, or both; population growth and declining mortality risk per age group	Huynen and Martens 2015
Skopje, Macedonia	Heat-related mortality	1986-2005; May - September	MRI-CGCM3; IPSL-CM5A-MR; GISS-E2-R	RCP8.5	2026-2045; 2081-2100	About 55 attributable deaths per year	Heat-related mortality would more than double in 2026-2045 to about 117 deaths	Heat-related mortality would more than quadruple in 2081-2100 to	Two models to project population growth; PM10	Martinez et al. 2016

Region	*Health outcome metric*	*Baselines*	*Climate model(s)*	*Scenario*	*Time periods of interest*	*Impacts at baseline*	*Projected impacts at 1.5°C*	*Projected impacts at 2°C*	*Other factors considered*	*Reference*
								about 245 deaths		
Japan, Korea, Taiwan, USA, Spain, France, Italy	Heat-related mortality for 65+ age group	1961-1990	BCM2	A1B	2030; 2050		In 2030, heat-related excess deaths increased over baselines in all countries, with the increase dependent on the level of adaptation	In 2050, heat-related excess deaths are higher than for 2030, with the increase dependent on the level of adaptation	Three adaptation assumptions: 0, 50, and 100%	Honda et al. 2014
Beijing, China	Heat-related mortality	1970-1999	Downscaled and bias corrected (BCSD) 31 GCMs in WCRP CMIP5; monthly change factors applied to daily weather data to create a projection	RCP4.5; RCP8.5	2020s (2010-2039), 2050s (2040-2069), 2080s (2070-2099)	Approximately 730 additional annual heat-related deaths in 1980s	In the 2020s, under low population growth and RCP4.5 and RCP8.5, heat-related deaths projected to increase to 1,012 and 1,019, respectively. Numbers of deaths are higher with medium and high population growth.	In the 2050s under low population growth, and RCP4.5 and RCP8.5, heat-related deaths projected to increase to 1,411 and 1,845, respectively Under a scenario of medium population and RCP8.5, by the 2080s, Beijing is	Adults 65+ years of age; no change plus low, medium, and high variants of population growth; future adaptation based on Petkova et al. 2014, plus shifted mortality 5%, 15%, 30%, 50%	Li et al. 2016

Region	*Health outcome metric*	*Baselines*	*Climate model(s)*	*Scenario*	*Time periods of interest*	*Impacts at baseline*	*Projected impacts at 1.5°C*	*Projected impacts at 2°C*	*Other factors considered*	*Reference*
								projected to experience 14,401 heat-related deaths per year, which is a 264.9% increase compared with the 1980s. Even with a 30% and 50% adaptation rate, the increase in heat-related death is approximately 7.4 times and 1.3 times larger than in the 1980s, respectively.		
Beijing, China	Cardiovascular and respiratory heat-related mortality	1971-2000	Access 1.0; CSIRO Mk3.6.0; GFDL-CM3; GISS E2R; INM-CM4	RCP4.5; RCP8.5	2020s; 2050s; 2080s	Baseline cardiovascular mortality 0.396 per 100,000; baseline respiratory mortality	Cardiovascular mortality could increase by an average percentage of 18.4% in the 2020s under RCP4.5 and	Cardiovascular mortality could increase by an average percentage of 47.8% and 69.0% in the, 2050s and		Li et al. 2015

Region	*Health outcome metric*	*Baselines*	*Climate model(s)*	*Scenario*	*Time periods of interest*	*Impacts at baseline*	*Projected impacts at 1.5°C*	*Projected impacts at 2°C*	*Other factors considered*	*Reference*
						0.085 per 100,000	by 16.6% under RCP8.5. Statistically significant increases are projected for respiratory mortality.	2080s under RCP4.5, and by 73.8% and 134% under RCP8.5. Similar increases are projected for respiratory mortality.		
Africa	Five thresholds for number of hot days per year when health could be affected, as measured by maximum apparent temperature	1961-2000	CCAM (CSIRO) forced by coupled GCMs: CSIRO; GFDL20; GFDL 21; MIROC; MPI; UKMO. CCAM was then downscaled. Biased corrected using CRU TS3.1 dataset	A2	2011-2040; 2041-2070; 2071-2100	In 1961-1990, average number of hot days (maximum apparent temperature $\geq$ 27C) ranged from 0 to 365, with high variability across regions.	In 2011-2040, annual average number of hot days (maximum apparent temperature $\geq$ 27C) projected to increase by 0-30 in most parts of Africa, with a few regions projected to increase by 31-50.	In 2041-2070, annual average number of hot days (maximum apparent temperature $\geq$ 27C) projected to increase by up to 296, with large changes projected in southern Africa and parts of northern Africa	Projected population in 2020 and 2025	Garland et al. 2015

Table S3.5 Projected vectorborne disease risks to human health

Region	Health outcome Metric	Baselines	Climate model(s)	Scenario	Time periods of interest	Impacts at baseline	Projected impacts at 1.5C	Projected impacts at 2C	Other factors considered	Reference
Malaria										
Global	Malarial distribution	1980-2009, 1980-2010	CMIP5, HadGem2-ES, IPSL-CM5A-LR, MIROC-ESM-CHEM, GFDL-ESM2M, NorESM1-M	RCP2.6; RCP4.5 RCP6.0 RCP8.5	2030s (2005 - 2035), 2050s (2035 - 2065), 2080s (2069 – 2099)	Before interventions, epidemic malaria widespread in mid-latitudes and some northern regions,	In the 2050s, length of the malaria transmission season increases over highland areas in most regions; however, the net effect on populations at risk relatively small in Africa, with large regional differences	In the 2080s, trends are more pronounced	Malaria models: LMM_RO, MIASMA, VECTRI, UMEA, MARA	Caminade et al. 2014
China	Human population exposed to 4 malarial vectors	Malarial records (2000-2010)	BCC-CSM1-1, CCCma_CanESM2, CSIRO-Mk3.6.0	RCP2.5, RCP4.5, RCP8.5	2030s ; 2050s	Exposure to *An. dirus* = 26.4 M; *An. minimus*= 162.8 M; *An. Lesteri* = 619.0 M; *An.*	In the 2030s, environmentally suitable area for two vectors increases by an average of 49% and 16%, under all	In the 2050s, environmentally suitable area for these vectors decreases by an average of 11% and 16%, with an		Ren et al. 2016

Region	Health outcome Metric	Baselines	Climate model(s)	Scenario	Time periods of interest	Impacts at baseline	Projected impacts at 1.5C	Projected impacts at 2C	Other factors considered	Reference
						sinensis = 1005.2 M	scenarios. Overall, a substantial increase in the population exposed.	increase of 36% and 11% for two other vectors. Increase in the population exposed larger than in the 2030s.		
Northern China	Spatial distribution of malaria	2004-2010	GCMs from CMIP3	B1, A1B, A2	2020; 2030; 2040; 2050	Average malaria incidence 0.107% per annum in northern China	In 2020, malaria incidence increases 19%-29%, and increases 43%-73% in 2030, with increased spatial distribution	In 2040, malaria incidence increases 33%-119% and 69%-182% in 2050, with increased spatial distribution	Elevation, GDP, water density index held constant	Song et al. 2016
Africa	Malaria transmission	1960-2005	CanESM2; IPSL-CM5A-LR; MIROC-ESM; MPI-ESM-LR	RCP2.6, RCP8.5	2030-2099		Over the period 2030-2099, increase in the regional extent and length of		Land use change	Tompkins et al. 2016

Region	Health outcome Metric	Baselines	Climate model(s)	Scenario	Time periods of interest	Impacts at baseline	Projected impacts at 1.5C	Projected impacts at 2C	Other factors considered	Reference
							transmission season, with greater impacts at RCP2.6 (temperatures can be too hot for malaria under RCP8.5)			
South and Southeast Asia	Malarial spatial pattern	1950-2000	MIROC-H	A2	2050, 2100	Malaria a risk in all countries		For 2050, a decrease in climate suitability in India (northern and eastern regions), southern Myanmar, southern Thailand, the region bordering Malaysia, Cambodia, eastern Borneo and the Indonesian	Eco-climatic index	Khormi et al. 2016

Region	Health outcome Metric	Baselines	Climate model(s)	Scenario	Time periods of interest	Impacts at baseline	Projected impacts at 1.5C	Projected impacts at 2C	Other factors considered	Reference
								islands. However, even if suitability decreases, most of the areas should remain conducive for the spread of malaria. Regions where climate suitability increases are southern and south-eastern mainland China and Taiwan. Similar but more extensive trends in 2100.		

Region	Health outcome Metric	Baselines	Climate model(s)	Scenario	Time periods of interest	Impacts at baseline	Projected impacts at 1.5C	Projected impacts at 2C	Other factors considered	Reference
Korea	Malaria	2001-2011	HadGEM3-RA based on HadGEM2-AO	RCP4.5	2011-2039, 2040-2069, 2070-2100	Malaria continues to regularly occur	In 2040-2069, the simulated time series indicated a slight increase in malaria, with a longer transmission season and early peak month for cases	In 2070-2100, the changes are larger		Kwak et al. 2014
South America	Malaria	Current	NASA GISS-E2-R, ENES HadGEM2-ES	RCP8.5	2070	25% of South America has a climate suitable for malaria (*P. falciparum*) transmission		In 2070, geographic range increases to 35% based on an increase in temperature of 2-3°C on average and a decrease in precipitation		Laporta et al. 2016
Aedes										

Region	Health outcome Metric	Baselines	Climate model(s)	Scenario	Time periods of interest	Impacts at baseline	Projected impacts at 1.5C	Projected impacts at 2C	Other factors considered	Reference
Global	Distributions of *Ae. aegypti* and *Ae. albopictus*	1950–2000	CMIP4 model projections: BCCR-BCM2.0, CSIRO-MK3.0, CSIRO-MK3.5, INM-CO3.0, MIROC medium resolution, NCAR-CCSM3.0	A2, B1, A1B	2050	Model predictions for the present day reflected the known global distributions of the two species		In 2050, projections indicated complex global rearrangements of potential distributional areas		Campbell et al. 2015
Global	Distribution of *Ae. aegypti*	1950-2000	CSIRO-Mk3.0, MIROC-H	A1B, A2	2030, 2070	Strong concordance between actual records and predicated conditions	In 2030, climatically favorable areas for *Ae. aegypti* globally projected to contract. Currently unfavorable areas, such as inland Australia, the Arabian Peninsula, southern Iran and parts of	In 2070, changes more pronounced.		Khormi et al. 2014

Region	Health outcome Metric	Baselines	Climate model(s)	Scenario	Time periods of interest	Impacts at baseline	Projected impacts at 1.5C	Projected impacts at 2C	Other factors considered	Reference
							North America may become climatically favorable			
Global and regional	Habitat suitability for the Asian tiger mosquito, a vector chikungunya, dengue fever, yellow fever and various encephalitides	2000-2009; ECHAM5/MESSy2	CMIP5: CCSM4, HadGEM2-CC, HadGEM2-ES, ISPL-CM5A-MR, MIROC5, MPI-ESM-LR, MRI-GCCM3, CSIRO-Mk3.60, EC-EARTH	A2, RCP8.5	2045-2054	*Ae. albopictus* habitat suitability index > 10% is 3,495 x10^6 individuals; for >70%, 1,788 x10^6 in a land area of 22 x 10^6 km2		For a habitat suitability index > 70%, approximately 2.4 billion individuals in a land area of nearly 20 million km2 potentially exposed to *Ae. albopictus*		Proestos et al. 2015
North America, United States	Climate suitability for *Ae. albopictus* vector for dengue, chikungunya, and vectorborne zoonoses such as West Nile	1981-2010	8 RCMs: CanRCM4, CRCM5, CRCM 4.2.3, HIRHAM5, RegCM3, ECPC, MM5I, WRF	RCP4.5, RCP8.5 A2	2020s (2011 – 2040), 2050s (2041 – 2070).	Index of precipitation and temperature suitability was highly accurate in discriminating suitable and non-	In 2011-2040 under RCP4.5, climate suitability increases across US, with the magnitude and pattern dependent on	In 2041-2070 under RCP4.5, areal extent larger than in earlier period; under 8.5, areal extent larger	Climatic indicators of *Ae. albopictus* survival; overwintering conditions (OW); OW combined with annual air temperature (OWAT); and an	Ogden et al. 2014a

Region	Health outcome Metric	Baselines	Climate model(s)	Scenario	Time periods of interest	Impacts at baseline	Projected impacts at 1.5C	Projected impacts at 2C	Other factors considered	Reference
	virus (WNV), Eastern Equine Encephalitis virus, Rift Valley Fever virus, Cache Valley virus and LaCrosse virus					suitable climate	parameter projected and RCM		index of suitability	
Southeastern USA	*Ae. aegypti* populations and dengue cases	1961-1990	GCM simulated baseline	A1B	2045-2065	Under baseline climate, dengue transmission may be possible in several sites in the southeast US		The potential for dengue transmission will continue to be seasonal throughout the southeastern US, without becoming a year-round phenomenon except perhaps in southern Florida that may have winter		Butterworth et al. 2016

Region	Health outcome Metric	Baselines	Climate model(s)	Scenario	Time periods of interest	Impacts at baseline	Projected impacts at 1.5C	Projected impacts at 2C	Other factors considered	Reference
								dengue activity. The length of the potential transmission season will increase for most sites		
Mexico	Dengue	1985-2007	National Institute of Ecology; added projected changes to historic observations	A1B, A2, B1	2030, 2050, 2080	National: 1.001/100.000 cases annually Nuevo Leon: 1.683/100.000 cases annually Queretaro: 0.042/100.000 cases annually Veracruz: 2.630/100.000 cases annually	In 2030, dengue incidence increases 12-18%	In 2050, dengue incidence increases 22-31%; in 2080, incidence increases 33-42% holding other factors constant	At baseline, population, GDP, urbanization, access to piped water	Colon-Gonzalez et al. 2013

Region	Health outcome Metric	Baselines	Climate model(s)	Scenario	Time periods of interest	Impacts at baseline	Projected impacts at 1.5C	Projected impacts at 2C	Other factors considered	Reference
Europe, Eurasia and the Mediterranean	Climatic suitability for Chikungunya outbreaks	1995-2007	COSMO-CLM, building on ECHAM5	A1B and B1	2011-2040, 2041-2070, 2071-2100	Currently, climatic suitability in southern Europe. The size of these regions will expand during the 21st century	In 2011-2040, increases in risk are projected for Western Europe in the first half of the 21st century	In 2041-2070, projected increased risks for central Europe. In 2071-2100, the highest risks projected for France, northern Italy and the Pannonian Basin. Many Mediterranean regions continue to be climatically suitable for transmission		Fischer et al. 2013
Europe	Potential establishment of *Ae. albopictus*	Current bioclimatic data derived from monthly	Regional climate model COSMO-CLM	A1B, B1	2011-2040, 2041-2070,		In 2011-2040, higher values of climatic suitability	Between 2011-40 and 2041-70, for southern		Fischer et al. 2011

Region	Health outcome Metric	Baselines	Climate model(s)	Scenario	Time periods of interest	Impacts at baseline	Projected impacts at 1.5C	Projected impacts at 2C	Other factors considered	Reference
		temperature and rainfall values			2071-2100		for *Ae. albopictus* increases in western and central Europe	Europe, only small changes in climatic suitability are projected. Increasing suitability at higher latitudes is projected for the end of the century.		
Europe	Dengue fever risk in 27 EU countries	1961-1990	COSMO-CLM (CCLM) forced with ECHAM5/MPI OM	A1B	2011-2040, 2041-2070, 2071-2100	Number of dengue cases are between 0 and 0.6 for most European areas, corresponding to an incidence of less than 2 per 100 000 inhabitants	In 2011-2040, increasing risk of dengue in southern parts of Europe	In 2041-2070, increased dengue risk in many parts of Europe, with higher risks towards the end of the century. Greatest increased risk around the	Socioeconomic variables, population density, degree of urbanization and log population	Bouzid et al. 2014

Region	Health outcome Metric	Baselines	Climate model(s)	Scenario	Time periods of interest	Impacts at baseline	Projected impacts at 1.5C	Projected impacts at 2C	Other factors considered	Reference
								Mediterranean and Adriatic coasts and in northern Italy		
Europe, and 10 cities in Europe with three reference cities in tropical and sub-tropical regions	Dengue epidemic potential for *Aedes* vectors	1901-2013	CRU-TS 3.22	RCP2.6, RCP4.5, RCP6.0,RCP8.5	2070–2099			In 2070-2099, increasing trends in intensity and duration for dengue epidemic potential along a south to north gradient. By the end of the century, dengue epidemic potential for *Ae. aegypti* could expand to northern Europe and up to eight months in		Liu-Helmersson et al. 2016

Region	Health outcome Metric	Baselines	Climate model(s)	Scenario	Time periods of interest	Impacts at baseline	Projected impacts at 1.5C	Projected impacts at 2C	Other factors considered	Reference
								southern Europe under RCP8.5		
Australia	Future dengue epidemic potential	1990–2011	CIMSiM, MPI ECHAM5	A2, B1	2046-2064	Dengue transmission possible in all study centers, with different transmission probability, depending on location and month		Under A2, decreased dengue transmission projected; some increases likely under B1		Williams et al. 2016
Queensland, Australia	Dengue outbreaks	1991-2011	MPI ECHAM 5 model	A2, B1	2046-2065		*Aedes aegypti* abundance increases under B1 16.6% and decreases 42.3% under A2; temperature increase of about 0.6°C			Williams et al. 2014

Region	Health outcome Metric	Baselines	Climate model(s)	Scenario	Time periods of interest	Impacts at baseline	Projected impacts at 1.5C	Projected impacts at 2C	Other factors considered	Reference
Guangzho, south-western China	Effects of seasonal warming on the annual development of *Ae. albopictus*	1980-2014	Mechanistic population model (MPAD), generating fifteen seasonal warming patterns	Fifteen seasonal warming patterns generated based on temperature increases from 0.5 to 5°C.			At an increase of 1°C, warming effects facilitate the development of species by shortening the diapause period in spring and winter. In summer, effects are primarily negative by inhibiting mosquito development; effects are mixed in autumn	Effects are more pronounced at an increase of 3°C.		Jia et al. 2017
New Caledonia	Dengue fever spatial heterogeneity	1995-2012	10 CMIP5 models: bcc-csm1-1, CanESM2, CCSM4, CNRM-CM5,	RCP4.5, RCP8.5	2010-2029, 2080-2099	24,272 dengue cases	In 2010-2029, under RCP8.5, average (across communes) dengue mean	By 2080-2099, if temperature increases by approximately 3°C, mean	Socioeconomic covariates	Teurlai et al. (2015)

Region	Health outcome Metric	Baselines	Climate model(s)	Scenario	Time periods of interest	Impacts at baseline	Projected impacts at 1.5C	Projected impacts at 2C	Other factors considered	Reference
			HadGEM2-CC, inmcm4, IPSL-CM5A-MR, IPSL-CM5B-LR, MPI-ESM-LR, NorESM1-M				annual incidence rates during epidemic years could raise by 29 cases per 10,000 people per year	incidence rates during epidemics could double. Under RCP8.5, the average dengue mean annual incidence rates during epidemic years could raise by 149 cases per 10,000 people per year		
Dhaka, Bangladesh	Weather variability impacts on dengue	2000-2010	Future monthly temperature was estimated by combining recorded baseline with projections	MMD-A1B	2100	Over study period, 25,059 dengue cases.		For a 2°C increase without adaptation, 2,782 additional dengue cases. For increase by 3.3°C, 16,030	1.3% increase in population	Banu et al. 2014

Region	Health outcome Metric	Baselines	Climate model(s)	Scenario	Time periods of interest	Impacts at baseline	Projected impacts at 1.5C	Projected impacts at 2C	Other factors considered	Reference
								additional cases by 2100		
Tanzania	Distribution of infected *Aedes aegypti* co-occurrence with dengue epidemics risk	1950-2000	CMIP5		2020, 2050	Currently high habitat suitability for *Aedes aegypti* in relation to dengue epidemic, particularly near water bodies	Projected risk maps for 2020 show risk intensification in dengue epidemic risks areas, with regional differences	In 2050, greater risk intensification and regional differences		Mweya et al. 2016
West Nile Virus										
North America	Geographic distribution of West Nile Virus (WNV)	2003–2011	USHCN, WorldClim, Seven GCMs, from the IPCC 4th assessment	A1B	2050-2060, 2080-2090			In 2050-2060, A northward and altitudinal expansion of the suitability of WNV, driven by warmer temperatures and lower		Harrigan et al. 2014

Region	Health outcome Metric	Baselines	Climate model(s)	Scenario	Time periods of interest	Impacts at baseline	Projected impacts at 1.5C	Projected impacts at 2C	Other factors considered	Reference
								annual precipitation; trends more pronounced in 2080		
USA	Population dynamics of three WNV vectors	1970-2000	LARS-WG, CCSM	A2, B1	2045-2065, 2080-2099			In both time periods, changes in mosquito population dynamics vary by location; mosquito activity periods expected to increase in the northern latitudes		Brown et al. 2015
Southern USA	*Cx. quinquefasciatus* (WNV vector) populations	1970-1999	USHCN, LARS-WG, AR4 GCM ensemble	A2	2021-2050	In the eastern USA, vector displays a latitudinal and elevational gradient		In 2021-2050, projected summer population depressions are most severe in the		Morin and Comrie 2013

Region	Health outcome Metric	Baselines	Climate model(s)	Scenario	Time periods of interest	Impacts at baseline	Projected impacts at 1.5C	Projected impacts at 2C	Other factors considered	Reference
								south and almost absent further north; extended spring and fall survival is ubiquitous. Projected onset of mosquito season is delayed in the southwestern USA; increased temperature and late summer and fall rains extend the mosquito season		
Canadian prairie provinces	Spatial and temporal distribution of *Cx.*	Monthly climatology data, 1961-1990;	Linear mixed model and generalized linear mixed	A2, A1B, B1	2020 (2010 – 2039),	Highest abundance *of Cx. tarsalis* occu		In 2050 under the median scenario, in		Chen et al. 2013

Region	Health outcome Metric	Baselines	Climate model(s)	Scenario	Time periods of interest	Impacts at baseline	Projected impacts at 1.5C	Projected impacts at 2C	Other factors considered	Reference
	tarsalis and WNV infection rate	abundance of *Cx. tarsalis* and WNV infection rate, 2005-2008	model used temperature and precipitation as the primary explanatory variables; NCAR-PCM run 2, MIMR, UKMO-HadGEM1		2050 (2040 – 2069) and 2080 (2070 – 2099)	rred in the southern Canadian prairies under baseline climate conditions and all future scenarios		current endemic regions, WNV infection rate increases 17.9 times. Abundance of *Cx. tarsalis* increases 1.4 times. Geographical distribution of *Cx. tarsalis* increases 33,195 km2 northward (1.6-fold).		
Europe, Eurasia, and the Mediterranean	Distribution of human WNV infection	Monthly temperature anomalies relative to 1980-1999, environmental variables for 2002-2013	NCAR CCSM3	A1B	2015-2050		In 2025, progressive expansion of areas with an elevated probability for WNV infections, particularly at the edges of	In 2050, increases in areas with a higher probability of expansion	Prevalence of WNV infections in the blood donor population	Semenza et al. 2016

Region	Health outcome Metric	Baselines	Climate model(s)	Scenario	Time periods of interest	Impacts at baseline	Projected impacts at 1.5C	Projected impacts at 2C	Other factors considered	Reference
							the current transmission areas			
Lyme disease and other tick-borne diseases										
North America (mainly Ontario and Quebec, Canada, and Northeast and Midwest, U.S)	Capacity of Lyme disease vector (*Ixodes scapularis)* to reproduce under different environmental conditions	1971–2010	CRCM4.2.3, WRF, MM5I , CGCM3.1, CCSM3	A2	1971-2000, 2011–2040, 2041–2070	In 1971–2010, reproductive capacity increased in North America increased consistent with observations	In 2011-2040, mean reproductive capacity increased, with projected increases in the geographic range and number of ticks	In 2041-2070, further expansion and numbers of ticks projected		Ogden et al. 2014b
Eastern U.S.	Lyme disease vector *Ixodes scapularis*	2001-2004	WRF 3.2.1	RCP4.5, RCP8.5	2057-2059	Peak Month and Peak Population had the greatest discriminatory ability across all life stages		Mean, median, and peak populations increase across most of the eastern U.S., with the largest increases under	10 dynamic population features	Dinghra et al. 2013

Region	Health outcome Metric	Baselines	Climate model(s)	Scenario	Time periods of interest	Impacts at baseline	Projected impacts at 1.5C	Projected impacts at 2C	Other factors considered	Reference
								RCP8.5; regions with the highest tick populations expanded northward and southward; season of questing adults increases in the south and decreases in the north		
U.S., 12 eastern states with > 90% of current cases	Lyme Onset Week (LOW)	1992–2007	5 AOGCMs from CMIP5	RCP2.6, RCP4.5, RCP6.0, RCP8.5	2025-2040, 2065-2080	LOW for 1992–2007 is 21.2 weeks	In 2025–2040, LOW is 0.4–0.5 weeks earlier, based on an increase in temperature of 1.2–1.7°, with regional differences. The largest	For 2065-2080, LOW is 0.7–1.9 weeks earlier, based on an increase in temperatures of 1.8–4.5°C, with regional differences.		Monaghan et al. 2015

Region	Health outcome Metric	Baselines	Climate model(s)	Scenario	Time periods of interest	Impacts at baseline	Projected impacts at 1.5C	Projected impacts at 2C	Other factors considered	Reference
							changes under RCP8.5	The largest changes under RCP8.5		
Southeastern US, NY	Emergence of *I. scapularis*, leading to Lyme disease	1994-2012			2050	19 years of tick and small mammal data (mice, chipmunks)	In the 2020s, the number of cumulative degree-days enough to advance the average nymphal peak by 4–6 days, and the mean larval peak by 5–8 days, based on 1.11–1.67°C increase in mean annual temperature	In the 2050s, the nymphal peak advances by 8–11 days, and the mean larval peak by 10–14 days, based on 2.22–3.06°C increase in mean annual temperature		Levi et al. 2017
Texas – Mexico transboundary region	Lyme disease transmission (*I. scapularis* with *B. burgdorferi*)	2011-2012 (for tick distribution)	CCCMA, CSIRO, HADCM3	A2A, B2A	2050	9% of tick samples were I. *scapularis*; 45% of these infected with		In 2050, habitat suitable for *I. scapularis* will remain relatively stable	MaxEnt model	Feria-Arroyo et al. 2014

Region	Health outcome Metric	Baselines	Climate model(s)	Scenario	Time periods of interest	Impacts at baseline	Projected impacts at 1.5C	Projected impacts at 2C	Other factors considered	Reference
						B. burgdorferi				
Southern Quebec (34 sites)	Risk of *Borrelia burgdorferi*, (bacteria causing Lyme disease in North America)	May to October 2011	CRCM 4.2.3, CMIP3 ensemble	A1b, A2, B1	2050	*Borrelia burgdorferi* detected at 9 of the 34 study sites. Risk ranged from 0.63 to 0.97, except in one site that was null)		In 2050, northern range of *B. burgdorferi* expands by approximately 250–500 km – a rate of 3.5–11 km per year		Simon et al. 2014
Europe	Climatic niche of *Ixodes ricinus*	1970-2010	CCCAMCGCM3.1-T47	A2, B2	2050; 2080	Current distribution of *Ixodes ricinus* is $3.1x10^6$ km^2	In 2050, increase of climatic niche of about 2-fold and higher climatic suitability under B2 than A2, both in latitude and longitude, including northern Eurasian regions (e.g.	In 2080, greater increase in climate suitability	Species distribution modeling	Poretta et al. 2013

Region	Health outcome Metric	Baselines	Climate model(s)	Scenario	Time periods of interest	Impacts at baseline	Projected impacts at 1.5C	Projected impacts at 2C	Other factors considered	Reference
							Sweden and Russia), that were previously unsuitable			
Europe	Climate suitability for ticks	1971-2010	IPSLCM5A-LR, MIROC-ESM-CHEM, GFDL-ESM2M, NorESM1-M	RCP2.6, RCP4.5, RCP6.0, RCP8.5	2050-2098	Seven of eight tick species exhibited strong climatic signals within their observed distributions		Varying degrees of northward shift in climate suitability for tick species with a climate signal, with the greatest shifts under the most extreme RCPs and later in the century		Williams et al. 2015
Other										
Continental portions of US and Mexico	Chagas disease; forecast the distribution of the host	1980-2012	CCCMA; CSIRO; HDCM3	A2, B2	2050	Present range of *T. gerstaeckeri*		In 2050, a northern and eastern shift of *T. gerstaeckeri*		Garza et al. 2014

Region	Health outcome Metric	Baselines	Climate model(s)	Scenario	Time periods of interest	Impacts at baseline	Projected impacts at 1.5C	Projected impacts at 2C	Other factors considered	Reference
	vector (*Triatoma gerstaeckeri* and *T. sanguisuga*)					= 1903784 km2 Present range of *T. sanguisuga* habitat = 2628902 km2		and a northern, eastern, and southern distributional shift of *T. sanguisuga*		
Venezuela	Chagas disease: number of people exposed to changes in the geographic range of five species of triatomine species	1950–2000	CSIRO3.0	A1B, B1	2020, 2060, 2080		In 2020 decreasing population vulnerability	In 2060, effects more pronounced, with less of a change under B1	MaxEnt model of climatic niche suitability	Ceccarelli & Rabinovich 2015
Venezuela and Argentina	Chagas Disease (vectors *Rhodnius prolixus* and *Triatoma infestans*)	1950–2000	HadGEM2-ES	RCP4.5, RCP6.0, RCP8.5	2050	4751 new cases of *Tr. cruzi* human infection annually in provinces at high-to-moderate		In 2050, heterogeneous impact on the climatic niches of both vector species, with a decreasing		Medone et al. 2015

Region	Health outcome Metric	Baselines	Climate model(s)	Scenario	Time periods of interest	Impacts at baseline	Projected impacts at 1.5C	Projected impacts at 2C	Other factors considered	Reference
						transmission risk		trend of suitability of areas that are currently at high-to-moderate transmission risk		
South America	Distributions of the vector and pathogen causing cutaneous leishmaniasis (*Lutzomyia flaviscutellata* and *Leishmania amazonensis*)	1950–2000	ACCESS1.0,BCC-CSM1.1, CCSM4, CNRM-CM5, GFDL-CM3, GISS-E2-R, HadGEM2-AO, HadGEM2-ES, HadGEM2-CC, INM-CM4, IPSL-CM5A-LR, MIROC5, MRI-CGCM3, MIROC-ESM-CHEM, MPI-ESM-LR, MIROC-ESM, NorESM1-M	RCP4.5, RCP8.5	2050	Occurrence of *L. flaviscutellata* included 342 presence records (277 from Brazil)		In 2050, pattern of climate suitability shifts, with expansion of regions with suitable climates, depending on model and RCP	Used two algorithms for each species datasets: presence only (BIOCLIM and DOMAIN), presence/background (MaxEnt and GARP), and presence/absence	Carvalho et al. 2015

Region	Health outcome Metric	Baselines	Climate model(s)	Scenario	Time periods of interest	Impacts at baseline	Projected impacts at 1.5C	Projected impacts at 2C	Other factors considered	Reference
South America	Range of vectors of leishmaniasis	1978-2007 vector data from Argentina, Brazil, Bolivia, Paraguay; 1960-1990 climate data	HadGEM2-ES	RCP4.5, RCP8.5	2050	Current range of *Lutzomyia intermedia* is 1,958,675 km2 and of *Lutzomyia neivai* is 2,179,175 km2		In 2050, *L. intermedia* mostly contracts in the southern part of its range by 41.1% (RCP4.5) or 46.8% (RCP8.5), perhaps with expansion in northeast Brazil; *L. neivai* mostly shifts its range southwards in Brazil and Argentina, with an overall contraction of 14.8% (RCP4.5) or 16.2% (RCP8.5)	Ecological niche modeling	McIntyre et al. 2017

Region	Health outcome Metric	Baselines	Climate model(s)	Scenario	Time periods of interest	Impacts at baseline	Projected impacts at 1.5C	Projected impacts at 2C	Other factors considered	Reference
Colombia	Visceral leishmaniasis caused by the trypanosomatid parasite *Leishmania infantum*	Present	CSIRO, Hadley	A2A, B2A	2020; 2050; 2080		In 2020, shift in the altitudinal distribution in the Caribbean Coast and increase in the geographic area of potential occupancy under optimistic scenario	In 2050, even greater geographic area of potential occupancy, with a greater impact under A2; the trends continue in 2080	MaxEnt model; three topographical variables	Gonzalez et al. 2013
Russian Federation, Ukraine, and Other Post-Soviet States	Geographical spreading and potential risk of infection of human dirofilariosis (zoonotic disease)	1981-2011	Russian Committee of Hydrometeorology		2030	In 1981 to 2011, 2154 cases of human dirofilariosis reported in the former USSR	By 2030, an increase of 18.5% in transmission area and 10.8% in population exposure		Growing degree-days (GDDs) matrix and SRTM digital elevation models to project 2030 estimates; constant population	Kartashev et al. 2014
Romania	Zoonotic disease risk as measures by the distribution of	present	CCSM4	RCP2.6, RCP4.5, RCP6.0, RCP8.5	2050, 2070	Range of *H. marginatum* = 97,992 km2;		In 2050, under all RCPs, range increases (range		Domsa et al. 2016

Region	Health outcome Metric	Baselines	Climate model(s)	Scenario	Time periods of interest	Impacts at baseline	Projected impacts at 1.5C	Projected impacts at 2C	Other factors considered	Reference
	thermophilic ticks (*H. marginatum* and *R. annulatus)*					Range of *R. annulatus* =28,181 km2		expansion and range shift) for both tick species, with the largest increase under RCP8.5; In 2070, mainly a range shift		
Baringo county, Kenya	Rift Valley Fever (RVF) virus vectors	2000	NOAA GFDLCM3	RCP4.5	2050	Lowlands highly suitable for all RVF vector species		In 2050, increase in the spatial distribution of *Cx. quinquefasciatus* and *M. africana* in highland and mid-latitude zones	Ecological niche modeling	Ochieng et al. 2016

Table S3.6 Projected health risks of undernutrition and dietary change associated with climate change

Region	*Health outcome metric*	*Baselines*	*Climate model(s)*	*Scenario*	*Time periods of interest*	*Impacts at baseline*	*Projected impacts at 1.5°C*	*Projected impacts at 2°C*	*Other factors considered*	*Reference*
Global and 21 regions	Undernutrition	1961-1990	BCM2.0; EGMAM1; EGMAM2; EGMAM3; CM4vl	A1B	2030; 2050		In 2030, 95,176 additional undernutrition deaths without adaptation and (ensemble mean) and 84,697 with adaptation under BCM2 scenario; Asia, and Sub-Saharan Africa, at highest risk	Risks are generally lower in 2050 in most regions because of underlying trends, significantly so under a high economic growth scenario.	Population growth; improved population health; crop models include adaptation measures	Hales et al. 2014
Global and 17 regions	Undernourished population; DALY (disability) caused by underweight of a child under 5 years of age	2005-2100	5 models from ISIMIP (GFDL-ESM2; NorESM1-M; IPSL-CM5A-LR; HadGEM2-ES; MIROC-ESM-CHEM)	RCP2.6 and 8.5 with SSP2 and SSP3	2005-2100	Baseline assumed no climate change (no temperature increase from present)	In 2050 under SSP3, global undernourished population is 530-550 million at 1.5 C. Global mean DALYs of 9.5 per 1000 persons caused by children underweight at 1.5 C.	In 2050 under SSP3, global undernourished population is 540-590 million a t 2.0 C. Global mean DALYs of 9.5 per 1000 persons caused by children underweight at 1.5 C.	Population growth and aging; Equity of food distribution;	Hasegawa et al. 2016

Region	*Health outcome metric*	*Baselines*	*Climate model(s)*	*Scenario*	*Time periods of interest*	*Impacts at baseline*	*Projected impacts at 1.5°C*	*Projected impacts at 2°C*	*Other factors considered*	*Reference*
Global divided into 17 regions	DALYs from stunting associated with undernutrition	1990-2008	12 GCMs from CMIP5	Six scenarios: RCP2.6 + SSP1; RCP4.5 + SSPs 1-3; RCP 8.5 + SSP2, SSP3	2005 - 2050	57.4 million DALYs in 2005	In 2030, DALYs decrease by 36.4 million (63%), 30.4 million (53%), and 16.2 million (28%) for SSP1, SSP2, and SSP3, respectively.	Further decreases in DALYsin 2050, to 11.6 million and 17.0 million for SSP1 and SSP2, respectively, and with an increase to 43.7 million under SSP3.	Future population and per capita GDP from the SSP database	Ishida et al. 2014
Global	Deaths associated with the impact of climate change on food production	1986-2005	International model for policy analysis of agricultural commodities and trade (IMPACT); purpose-built global health model estimated changes in mortality associated with changes in dietary and weight-related risk factors, focusing on changes in the	RCP 8.5 + SSP2; RCPs 2.6, 4.,5 and 6.0 plus SSPs 1 and 3 for sensitivity analyses	2050			By 2050, per-person reductions of 3·2% (SD 0·4%) in global food availability, 4·0% (0·7%) in fruit and vegetable consumption, and 0·7% (0·1%) in red meat consumption. These changes associated with 529 000 climate-related deaths worldwide (95% CI 314 000–736 000). Twice as many deaths	Projected changes in population and GDP; increases in food availability and consumption in the reference scenario without climate change resulted in 1·9 million avoided deaths (95% CI 0·9–2·8 million) in 2050	Springmann et al. 2016

Region	*Health outcome metric*	*Baselines*	*Climate model(s)*	*Scenario*	*Time periods of interest*	*Impacts at baseline*	*Projected impacts at 1.5°C*	*Projected impacts at 2°C*	*Other factors considered*	*Reference*
			consumption of fruits and vegetables, and red meat, and on changes in bodyweight associated with changes in overall caloric availability; HADGEM2-ES, ISPL-CM5A-LR, MIROC-ESM_CHEM					associated with reductions in fruit and vegetable consumption than in climate-related increases in underweight. Highest risks projected in southeast Asia and western Pacific.	compared with 2010. Climate change reduced the number of avoided deaths by 28% (95% CI 26–33).	